



7-29-2022

## Resonant Energy Exchange in Ultracold Rydberg Atoms


Samantha Grubb

*Ursinus College*, [sagrubb@ursinus.edu](mailto:sagrubb@ursinus.edu)

Alan Okinaka

*Ursinus College*, [alokinaka@ursinus.edu](mailto:alokinaka@ursinus.edu)

Follow this and additional works at: [https://digitalcommons.ursinus.edu/physics\\_astro\\_sum](https://digitalcommons.ursinus.edu/physics_astro_sum)

 Part of the [Atomic, Molecular and Optical Physics Commons](#), and the [Quantum Physics Commons](#)  
[Click here to let us know how access to this document benefits you.](#)

---

### Recommended Citation

Grubb, Samantha and Okinaka, Alan, "Resonant Energy Exchange in Ultracold Rydberg Atoms" (2022).  
*Physics and Astronomy Summer Fellows*. 42.  
[https://digitalcommons.ursinus.edu/physics\\_astro\\_sum/42](https://digitalcommons.ursinus.edu/physics_astro_sum/42)

This Paper is brought to you for free and open access by the Student Research at Digital Commons @ Ursinus College. It has been accepted for inclusion in Physics and Astronomy Summer Fellows by an authorized administrator of Digital Commons @ Ursinus College. For more information, please contact [aprock@ursinus.edu](mailto:aprock@ursinus.edu).

RESONANT ENERGY EXCHANGE IN ULTRACOLD  
RYDBERG ATOMS

by

Samantha Grubb and Alan Okinaka

Department of Physics  
Ursinus College

July 30, 2022



Copyright © July 30, 2022 by Samantha Grubb and Alan Okinaka  
All rights reserved



# Abstract

Ultracold Rydberg atoms serve as good systems in which resonant dipole-dipole interactions can be observed. The goal of our work is to design a simulation in which energy exchange among many nearly evenly spaced energy levels is observed. These observations are useful for understanding the time evolution of complicated quantum systems, and have applications in quantum computing and simulating. We are utilizing a supercomputer to run our simulation as well as studying the system experimentally. Once we obtain simulated results, we plan to compare them with the results obtained in a lab.



# Contents

<b>Abstract</b>	<b>iii</b>
<b>List of Figures</b>	<b>vii</b>
<b>1 Introduction</b>	<b>1</b>
1.1 Rydberg Atoms and the Stark Effect . . . . .	2
<b>2 Experiment</b>	<b>5</b>
<b>3 Model</b>	<b>7</b>
3.1 Simple Case . . . . .	7
3.2 Larger Systems . . . . .	10
<b>4 Results</b>	<b>13</b>
<b>5 Conclusion</b>	<b>17</b>
<b>A Appendix</b>	<b>19</b>





# List of Figures

1.1	The $n = 34$ manifold including $m_j = 0.5, 1.5,$ and $2.5$ . . . . .	4
2.1	Probability distribution the spikes showing the electrons that were detected after ionization. . . . .	5
2.2	Depiction of magneto optical trap (MOT) . . . . .	6
3.1	Analysis of dipole-dipole interaction in a two atom three level system.	8
3.2	Analysis of dipole-dipole interaction in a two atom six level system.	11
4.1	Evolution of the probability of 27 states as a function of time, where the initial state is in the middle. . . . .	14
4.2	Experimental and simulated data. . . . .	15
4.3	Simulated results compared to frequency scan across energy levels.	16



# Chapter 1

## Introduction

The quantum dynamics in complex interacting systems is currently an intense field of research. One example of these complex systems are solid state systems. Solid state systems have many particles and a complex energy structure. While their dynamics cannot be simulated on classical computers, they can potentially be simulated on quantum analog simulators. This would grant an increased understanding of these types of systems [1].

Rydberg, or highly excited atoms, are excellent candidates for quantum analog computers. This is because they interact strongly with each other and weakly with the environment [2]. They are also ultra-sensitive to electric and magnetic fields, and exhibit the Stark effect. This occurs when the energy levels of an atom shift in the presence of an electric field [3]. These atoms can be cooled in a magneto-optical trap (MOT) to temperatures as low as a few hundred  $\mu\text{K}$ . This results in a frozen Rydberg gas, in which the Rydberg atoms can be treated as stationary. After this, they are left to interact for a few microseconds [4].

These ultracold atoms interact with each other via dipole-dipole interactions. Previous studies have modeled systems with a few energy levels. Anderson *et al.* observed the  $25s_{1/2} + 33s_{1/2} \rightarrow 24p_{1/2} + 34p_{3/2}$  resonances in a MOT [4]. Altieri *et al.* has observed several similar interactions [5]. Recently, Liu *et al.* measured the

time evolution of three and four-body dipole-dipole interactions [6]. We simulated and observed this energy transfer in more complicated systems within the Stark manifold.

In order to conduct the experiment, we utilized a MOT. Figure 1.1(a) shows the specific  $n = 34$  manifold that we studied along with the excitation and detection process. The atoms are excited with a laser to Rydberg states, shown by the red line below the center of the manifold. From here, they are left to interact: the two red arrows in the blue box show an example of a dipole-dipole interaction involving evenly spaced energy levels within the Stark manifold. After this, a microwave probe excites the atoms to the  $36d$  state for detection.

Utilizing a supercomputer, we designed a model to study the presence of dipole-dipole interactions in these complicated systems. In contrast to previous studies, we were able to generate results for systems with tens of energy levels. Fig. 1.1(b) shows an example of the specific energy levels we used when studying the dynamics of this interaction. In several cases, we observed an asymmetry in the amount of population above and below the initial state. We also observed states beginning to populate at different times. Furthermore, the simulated results were compared with obtained experimental data, and the two showed good qualitative agreement.

## 1.1 Rydberg Atoms and the Stark Effect

Rydberg atoms are atoms that have an outermost electron with large principle quantum number  $n$  [2]. These highly excited atoms are much larger than typical atoms. They also have exaggerated properties since they have a weakly attached valence electron. More specifically, they are highly susceptible to electric and magnetic fields.

When an electric field is applied to Rydberg atoms, they exhibit the Stark effect. The Stark effect is the shift in the energy levels of an atom when an electric field is applied. The energy levels in Rydberg atoms fan out and produce complicated systems because of their many degenerate states and large size. We see an example of these energy states fanning out in Fig. 1.1(a). This is referred to as a Stark map, or manifold, in which dipole-dipole interactions can occur.

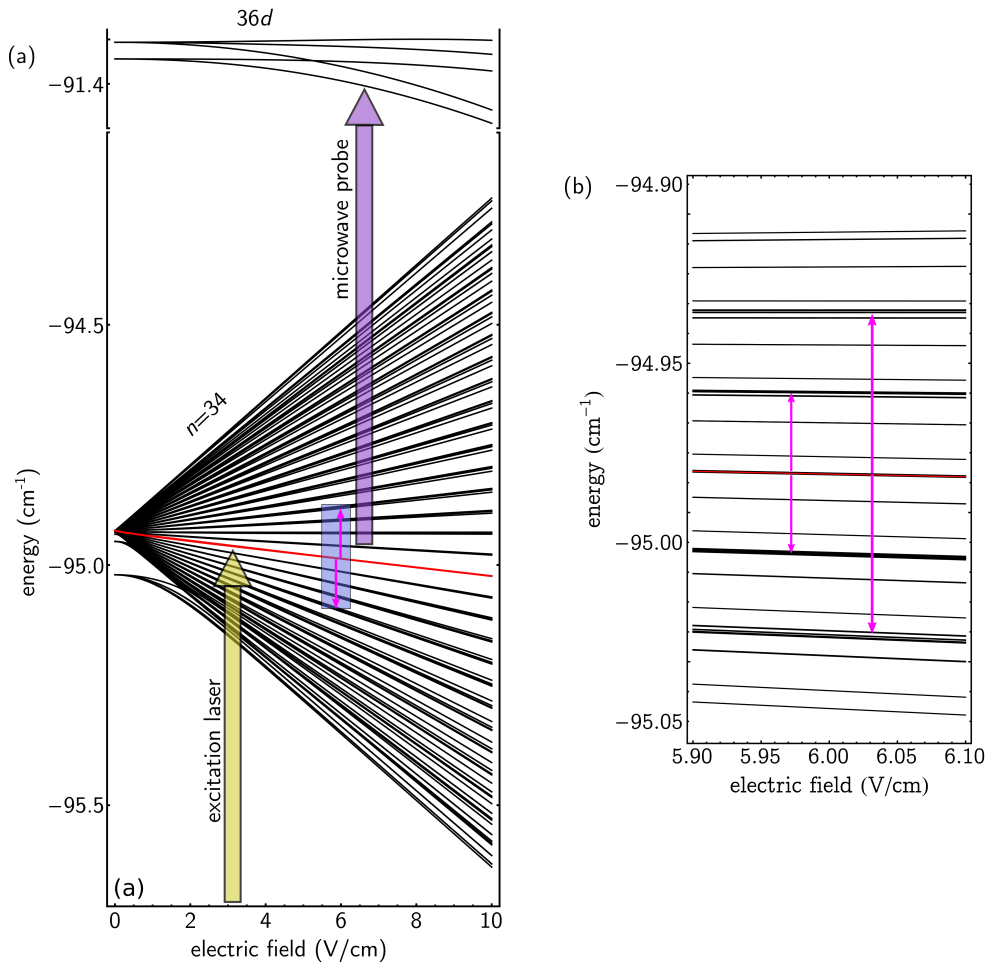


**Figure 1.1:** The  $n = 34$  manifold including  $m_j = 0.5, 1.5,$  and  $2.5$ . (a) In the experiment we excite the atoms with a laser to the red energy level dipole-dipole interaction ensues, and the microwave pulse excites the atoms to the  $36d$  state for detection. (b) Close up of the highlighted 55 energy levels that are included in the simulation. The initial state is shown in red. The close up shows the  $m_j = 0.5, 1.5, 2.5, 3.5,$  and  $4.5$ .

# Chapter 2

## Experiment

The experiment uses a MOT as shown in Fig. 2.2(a) which is a vacuum with lasers trapping rubidium atoms in a gas. We use rubidium since there is one outer shell electron which we can easily excite to high energy levels. We excite the rubidium atoms to the Rydberg state with a 776 nm and a 1265 nm laser model shown in Fig. 2.2(b). Also we cool the atoms close to a few hundred micro kelvin so that they are moving very slowly. Since the atoms don't have a big change in position then we can approximate them as stationary.

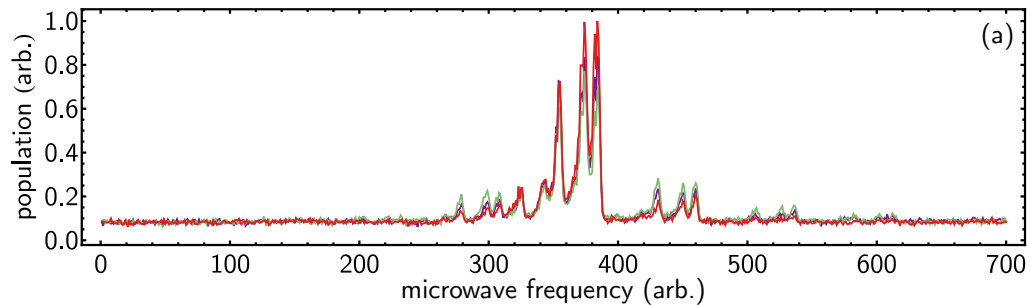


**Figure 2.1:** (a) Probability distribution the spikes showing the electrons that were detected after ionization.

Now that we have the atoms excited to the Rydberg state we wait a few microseconds for dipole dipole interactions to occur. Then we apply an microwave field pulse to excite a particular manifold state to the  $36d$ . The electric field ramp is applied. This increases with time so that it ionizes any atoms in the  $36d$  before



the manifold. The electric field then excites the electrons towards our detector.

We go through this process multiple times and then average the data to get a final probability distribution of the Rydberg atoms' energy level. The microwave spectrum is shown in Fig. 2.1. Peaks lower in the microwave frequency were higher in the manifold. The tallest peak in the middle is the initial state which is composed of five states in the  $36d$ . These five states are due to the five energy levels that fan out from the  $36d$ . Earlier in time shown in red the initial state has high population. Later in time in green the initial state decreases in population. The other states increase in population as time advances.

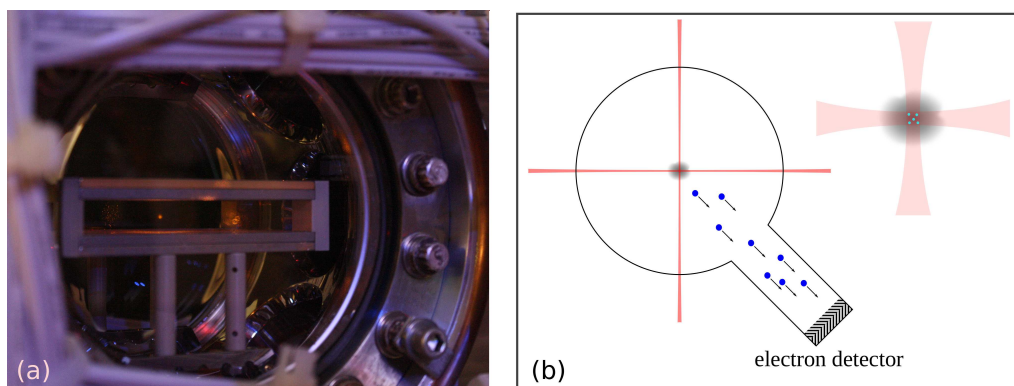


**Figure 2.2:** Depiction of MOT (a) Picture of the MOT. (b) MOT showing the trapped Rydberg atoms. A large electric field is applied to ionize the atoms and send the electrons to the detector. The zoom in shows where the two red excitation beams cross and excite Rydberg atoms.

# Chapter 3

## Model

### 3.1 Simple Case

Consider a system with 3 energy levels and 2 atoms shown in Fig. 3.1(a). In this case, both atoms start at energy level 0. One atom rises to energy level 1, and the other drops to the -1 level. This exhibits a two-body dipole dipole interaction. In order for interaction to occur, two Rydberg atoms' electrons must be between two equidistant energy levels. Two atoms initially in the 0 level can exchange energy by

$$m_0 + m_0 \leftrightarrow m_1 + m_{-1}. \quad (3.1)$$

Our goal is to solve for the time evolution of this system. The first step is to list all of the possible states that conserve energy. For the system shown in 3.1(a), the states are

$$\phi_0 = |0, 0\rangle \quad (3.2)$$

$$\phi_1 = |-1, 1\rangle \quad (3.3)$$

$$\phi_2 = |1, -1\rangle, \quad (3.4)$$

where the first element in the ket is the energy level of the first atom, and the second

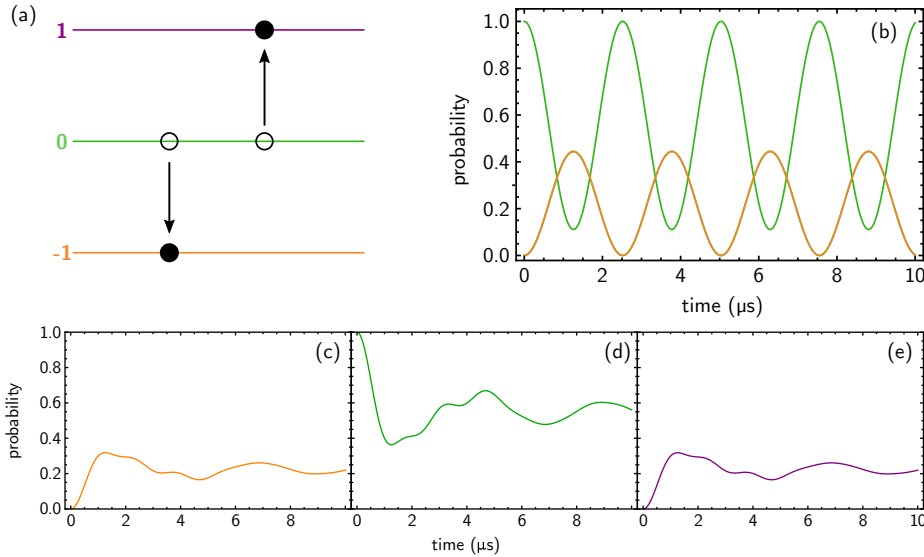


**Figure 3.1:** Analysis of dipole-dipole interaction in a two atom three level system. (a) Depiction of dipole-dipole interaction in a system with three energy levels and two atoms. The first (orange line) and third (purple line) energy levels are evenly spaced from the initial level (green line). (b) Probability plotted as a function of time over ten microseconds displaying each of the three energy levels shown previously. (c) Probability of atom being in the first energy level, (d) the initial state, and (e) the second energy level in which the positions are randomized and the results are averaged over one hundred runs.

element is the energy level of the second atom.

After we have our list of states we can calculate our Hamiltonian matrix

$$\hat{H} = \begin{pmatrix} E_0 & \alpha & \alpha \\ \alpha & E_1 & 0 \\ \alpha & 0 & E_2 \end{pmatrix}. \quad (3.5)$$

We can obtain the elements of our Hamiltonian matrix using  $\langle -1, 1 | \rho | 0, 0 \rangle = \alpha = \frac{\mu\nu}{R^3}$ .  $\mu$  and  $\nu$  are the dipole moments,  $\rho$  is the dipole operator, and  $R$  is the distance between the two atoms.

These matrix elements can be simplified by subtracting the initial energy levels from the diagonals. This results in detunings, which are defined as  $\delta_n = E_n - E_0$ .

$E_n$  is the energy level of the  $n$ th state and  $E_0$  is the energy level of the initial state. Since the energy levels are evenly spaced, the detunings with respect to the initial state become zero. Since there is a difference in energy between the remaining diagonals, the detunings become  $\delta_n$ . Therefore, our Hamiltonian becomes

$$\hat{H} = \begin{pmatrix} 0 & \alpha & \alpha \\ \alpha & \delta_1 & 0 \\ \alpha & 0 & \delta_2 \end{pmatrix}. \quad (3.6)$$

After we create the Hamiltonian, we calculate the time evolution operator. We can calculate the state at time  $t$  utilizing

$$\psi(t) = \hat{S}\hat{\Lambda}(t)\hat{S}^\dagger\psi(0). \quad (3.7)$$

$\hat{S}$  is a matrix of the eigenvectors that results from diagonalizing the Hamiltonian and  $S^\dagger$  is the conjugate transpose of that matrix.  $\hat{\Lambda}(t)$  is a diagonal matrix with  $\hat{\Lambda}_{ii} = e^{-i\lambda t}$ , where  $\lambda_n$  is the  $n$ th eigenvalue, and  $\psi(0)$  is the initial state.

Now we can use that time evolution operator to calculate the probabilities at different levels. The sinusoidal waves that can be seen in 3.1(b) are called Rabi oscillations. This shows the probabilities oscillating between the initial state (green) and the other states (orange). Throughout time the probabilities between the initial state and the other states add up to one. Figure 3.1(c-e) shows the probabilities of each state individually. The initial state (green) decreases as time goes on and the other states (orange and purple) start to populate symmetrically.

## 3.2 Larger Systems

Now consider a larger system with four atoms and six energy levels. Using this system, we can illustrate complicated dynamics that can arise within the manifold. For example, we can see an asymmetry in the amount of electrons above and below the initial state. This asymmetry is shown in Fig. 3.2(a), where the energy levels below the initial state have more electrons than the energy levels above the initial state.

This asymmetry develops in the following way. In the leftmost panel in Fig. 3.2(a), four atoms start at level 0. Two move to level 1 and the remaining two move to level -2. In the central panel, a dipole-dipole interaction occurs between the two atoms at level 1: one moves to level 2 and the other moves to level -1. Finally, this results in the rightmost panel depicting a system in which energy levels below the initial state have three electrons, and the energy levels above the initial state have one.

In order to make our model more similar to the experiment, we have tried to utilize as many energy levels as we can. Our simulation can accommodate up to four atoms and tens of energy levels which produces thousands of states and outputs a Hamiltonian with a rank that can be larger than 100,000. Since this involves solving a very large matrix, we have to use a supercomputer.

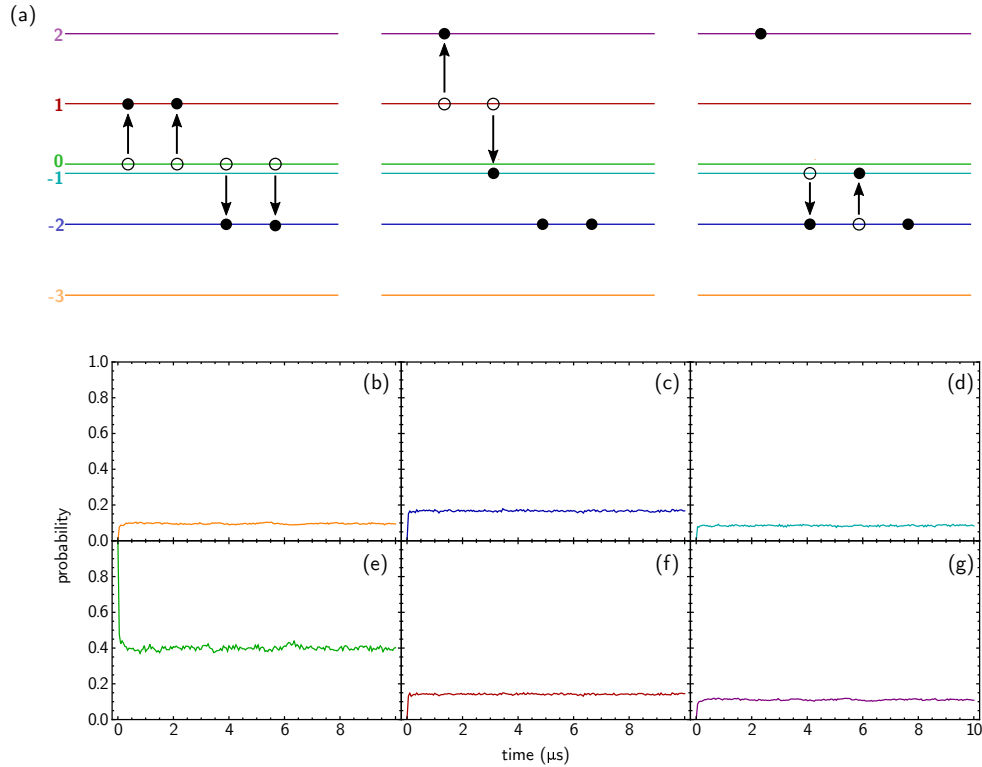


**Figure 3.2:** Analysis of dipole-dipole interaction in a two atom six level system. (a) Depiction of dipole-dipole interaction (left to right). In this case, the levels are not all evenly spaced. However, the second (dark blue line) and fifth (dark red line) energy levels are evenly spaced from the initial level (green line). Additionally, the first (orange line) and sixth (purple line) energy levels are evenly spaced from the initial level. Despite the asymmetry, it is important to note that the third (teal line) and sixth energy levels are evenly spaced from the initial level. This allows the third level to be populated even though it does not have a symmetric pairing like the other levels do. This energy transfer results in an asymmetry in the percent of population in the states above and below the initial state. There is also an always-resonant interaction depicted in the third diagram. (b) Probability of atom being in the first, (c) second, (d) third, (e) initial, (f) fourth, and (g) fifth energy level in which the positions are randomized in a cube and the results are averaged over fifty runs. Energy level -1 has significant population in it as shown in (d), but has no symmetric partner.



# Chapter 4

## Results

We ran our simulation on a supercomputer for many different cases, utilizing energy levels within specific parts of the  $n = 34$  manifold displayed in Fig. 1.1(a). These simulated results were also compared to experimental results.

We analyzed the time evolution of the central 27 states in Fig. 1.1(b). The simulation had four atoms that were randomly arranged in a sphere. In Fig. 4.1, each horizontal row on the y axis represents a different energy level, with the initial energy level being in the center. Warmer colors represent higher probabilities and cooler colors represent lower probabilities. The initial level can be seen starting at red and dropping off to orange as it loses population in the other levels due to dipole-dipole interactions.

Additionally, there is an asymmetry in the population of levels above and below the initial level. The two levels immediately above the initial level end up yellow, with probabilities around 0.07. However, there is no yellow below the initial level except for early times.

The levels also begin to populate at different rates. For example, the top two levels both begin at blue, but the topmost level increases from black to blue to green more quickly than the level below it. This is also apparent at numerous other levels on the graph.



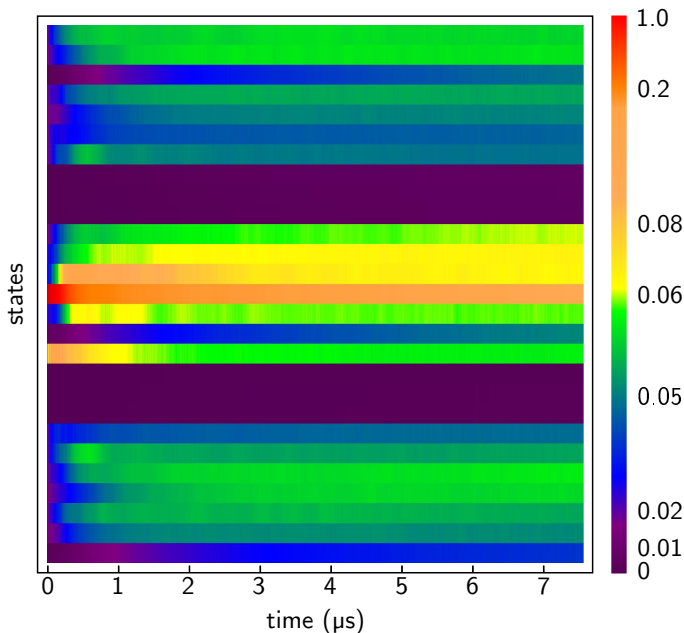


**Figure 4.1:** (a) Evolution of the probability of 27 states as a function of time, where the initial state is in the middle. Warmer colors indicate a higher probability and cooler colors indicate lower probability. The asymmetry in the population of states above and below the initial state is apparent, with more population being below the initial state. Despite this asymmetry, there is still an equal amount of energy above and below the initial state due to conservation of energy. Each energy level starts populating at a different starting time as well.

The simulated data was also compared to the experimental data obtained in a lab as shown in Fig. 4.2. Differing energy levels are represented by different colors. Fig. 4.2(a) depicts the electron population as a function of time, and Fig. 4.2(b) depicts the probability as a function of time, both for 55 energy levels within the Stark manifold. The initial energy level is shown in blue, and in both cases, is fully populated at  $t = 0$  but drops off over time. The remaining levels populate increasingly over time. Many of the energy levels appear to have symmetric pairs above and below the initial state. For example, the orange level below the initial state and red level above increase rapidly and then level out as time goes on.

In Fig. 4.3, the population of levels over time are displayed as a function of

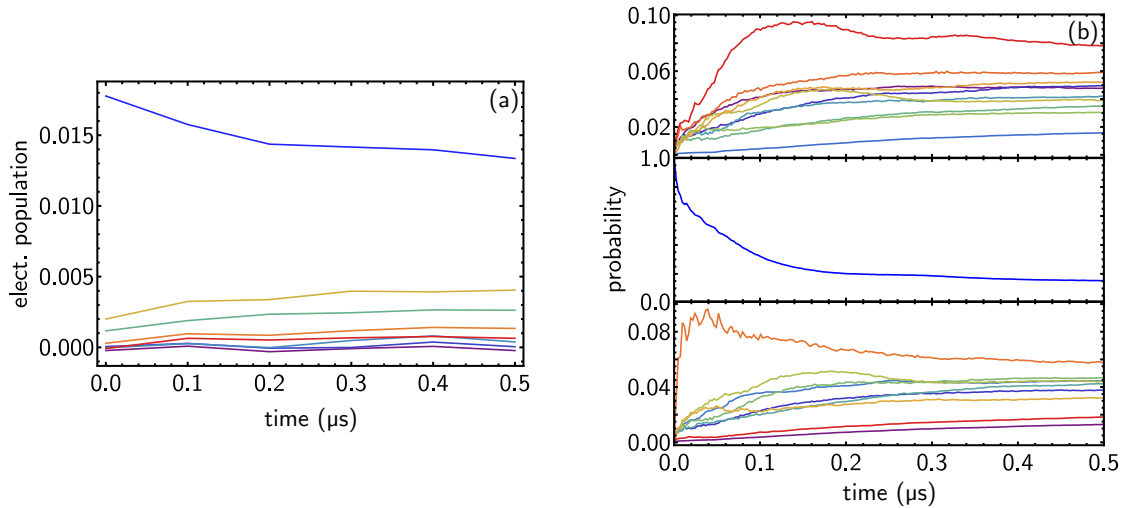


**Figure 4.2:** Experimental and simulated data. (a) Experimental data showing the electron population in a variety of energy levels. (b) Simulation data showing the probability of finding the atom in a variety of energy levels. The middle panel of b highlights the initial state while the lower panel shows energy levels below the initial state and the upper panel shows energy levels above the initial state.

microwave frequencies. Figure 4.3(a) shows the experimental data and Fig. 4.3(b) shows the simulated data. In both cases, the initial state is shown through the peak in the center, and the remaining probability can be seen distributing to different states. In the experimental data, more peaks in population are evident closer to the initial state. This is qualitatively similar to what we see in the simulated results.

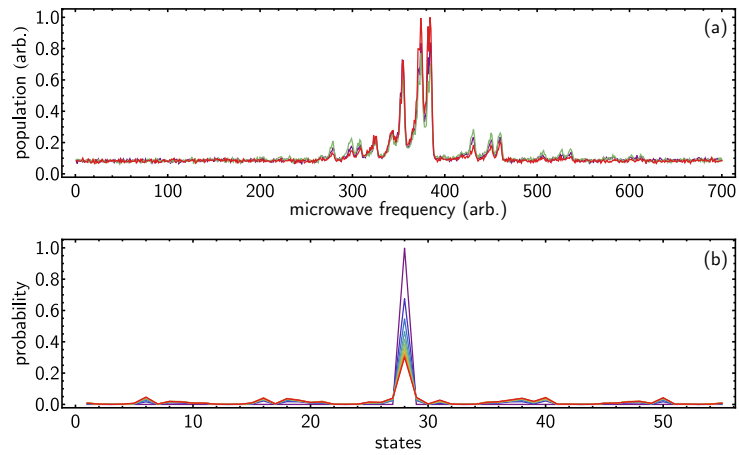


**Figure 4.3:** Simulated results compared to frequency scan across energy levels. (a) Frequency scan across the energy levels that we chose to study in the manifold. The peaks show the electron population as a function of microwave frequency, detected at the d state with our channel plate charge detector. (b) Probability of the atom being in each state. Each color shows a different time. The initial state is the highest peak in the middle.

# Chapter 5

## Conclusion

Our simulations show energy spreading from the initial state on a timescale that is qualitatively similar to experimental results. In the future, we would like to observe more specific similarities between the simulated and experimental results.

For example, we would like to obtain results at different starting points in the manifold and analyze them in comparison to the experimental results. Furthermore, we are currently using artificial dipole moments when running the simulation. We would like to use actual dipole moments going forward to hopefully obtain more accurate results. Additionally, our simulation suggests that there is an asymmetry in the states populated above and below the initial state. We would like to observe similar patterns in the lab. Another goal is to alter the way we obtain the possible energy states for our simulation. We are currently analyzing only the states with small detunings. We would like to see if including other possible states would affect the probability distribution of our results.



# Appendix A

Throughout this research, we utilized numerous Mathematica files. These files can be found in the "Summer 2022 Appendix Files" folder in Microsoft Teams. Below is a list of the files we used and their descriptions.

1. **examplecases.nb** Used to generate examples in model section: 2 atoms 3 levels, and 4 atoms 6 levels. Works for smaller cases and allows for the input of specific energy levels.
2. **full-simulation.nb** Full simulation used to calculate preliminary results prior to use of supercomputer.
3. **matrix-sizes.nb** Exports files including the sizes of the matrices for different cases. Helpful for understanding how long supercomputer run will take.
4. **supercomputer-data-analysis.nb** Used to analyze data obtained from supercomputer.
5. **colorcodedstarkmap.nb** Provides depictions of stark map and highlights different parts of the manifold.
6. **manifold-manifold-Simulation-Culling levels.nb** Full simulation in which certain states can be culled out.
7. **mapLoader-sa.nb** Generates Stark manifold and list of energies.

**8. manifold-manifold-Simulation-Comments.nb** Full manifold-manifold simulation with comments.

**9. experimental-data.nb** Analysis of data obtained in the lab at Bryn Mawr.

\*Some of these files may require you to change file pathways

# Bibliography

- [1] D. Jaksch, J. I. Cirac, P. Zoller, S. L. Rolston, R. Côté, and M. D. Lukin. Fast quantum gates for neutral atoms. 85(10):2208–2211. Publisher: American Physical Society.
- [2] Thomas F. Gallagher. *Rydberg Atoms*. Cambridge University Press.
- [3] Daniel Kleppner, Michael G. Littman, and Myron L. Zimmerman. Highly excited atoms. 244(5):130–149. 45 citations (Crossref) [2022-06-07] Publisher: Scientific American, a division of Nature America, Inc.
- [4] W. R. Anderson, J. R. Veale, and T. F. Gallagher. Resonant dipole-dipole energy transfer in a nearly frozen rydberg gas. 80(2):249–252.
- [5] Emily Altieri, Donald P. Fahey, Michael W. Noel, Rachel J. Smith, and Thomas J. Carroll. Dipole-dipole interaction between rubidium rydberg atoms. 84(5):053431. 19 citations (Crossref) [2022-06-07].
- [6] Zhimin Cheryl Liu, Nina P. Inman, Thomas J. Carroll, and Michael W. Noel. Time dependence of few-body f<sup>l</sup>’orster interactions among ultracold rydberg atoms. 124(13):133402. 3 citations (Crossref) [2022-06-07] Publisher: American Physical Society.



